International Journal of Biological and Pharmaceutical Sciences Archive

ISSN: 0799-6616 (Online)

Journal homepage: https://ijbpsa.com/

(RESEARCH ARTICLE)

Check for updates

DEVELOPMENT AND CHARACTERISATION OF A PH-RESPONSIVE, COLOUR-CHANGING CMC–PVA BIOPOLYMER FILM WITH INTEGRATED GLUCOSE-SENSING CAPABILITY FOR VISUAL MONITORING OF WOUND INFECTION

Nallagandla Rajitha [1,*], Bonthapally Vaishali [2], Auti Vineetha [2], Harika Guduguntla [2], Vishnubakthula Manogna [2] and Hechhu. Ramana [3]

[1] Department of Pharmaceutics, Malla Reddy Institute of Pharmaceutical Sciences, Malla Reddy Vishwavidyapeeth (Deemed to be University), Maisammaguda, Dulapally, Secunderabad Hyderabad 500100, Telangana, India.
[2] Pharm D 3rd Year Students from Malla Reddy Institute of Pharmaceutical Sciences, Malla Reddy Vishwavidyapeeth (Deemed to be University), Maisammaguda, Dulapally, Secunderabad Hyderabad 500100, Telangana, India.
[3] Department of Pharmaceutical Chemistry, Malla Reddy Institute of Pharmaceutical Sciences, Malla Reddy Vishwavidyapeeth (Deemed to be University), Secunderabad, 500100, Telangana;
* Corresponding Author

ORCID Details
Nallagandla Rajitha: https://orcid.org/0009-0000-7396-6664

International Journal of Biological and Pharmaceutical Sciences Archive, 2026, 12(02), 126–136

Publication history: Received on 29 September 2026; revised on 05 November 2026; accepted on 07 November 2026

Article DOI: https://doi.org/10.53771/ijbpsa.2026.12.2.0110

Copyright © 2026 Author(s) retain the copyright of this article. This article is published under the terms of the Creative Commons Attribution License 4.0

ABSTRACT

Wound pH shifts from the mildly acidic range of healing tissue (pH 4.0–6.0) to alkaline values (pH 7.0–9.0) during infection, often before overt clinical signs appear. Dressings that report this change visually could allow earlier intervention without removing the dressing.

Objective: To develop and characterize a pH-responsive, colour-changing carboxymethyl cellulose (CMC)–polyvinyl alcohol (PVA) film containing red cabbage anthocyanin and curcumin as a dual-dye indicator, and to integrate a low-cost glucose-sensing layer.

Methods: Three citric acid cross-linked films (F1, F2 and F3; CMC:PVA 1:2, 1:1 and 2:1) were prepared by solvent casting with glycerol and PEG-400 as plasticizers and alum as dye mordant. Dye pH response was recorded across pH 4–9. Films were evaluated for thickness, swelling in phosphate-buffered saline (PBS), and inhibition of heat-induced albumin denaturation as an in vitro anti-inflammatory screen. The F2 film was modified with an alginate–phenol red glucose-sensing layer (F2-BIO) cross-linked with $CaCl_2$ and coated with chitosan. Anti-biofilm activity against *Escherichia coli* was assessed by crystal violet assay.

Results: colour transitions across pH 4–9; thickness and swelling of F1–F3; % denaturation inhibition of F2 versus diclofenac; glucose-dependent colour change of F2-BIO; reduction in biofilm absorbance at 570 nm.]

Conclusion: The platform combines a visual pH read-out with a glucose channel in an inexpensive biopolymer matrix and offers a basis for smart wound dressings.

Keywords: Smart Wound Dressing; pH Indicator; Anthocyanin; Curcumin; Carboxymethyl Cellulose; Polyvinyl Alcohol; Glucose Biosensor; Biofilm.

1 INTRODUCTION

Chronic and infected wounds impose a considerable clinical and economic burden, and conventional dressings give no information about the state of the wound bed. Infection is usually recognized late, through erythema, exudate, odour or pain, and assessing it normally requires removing the dressing, which disturbs healing and risks contamination. Dressings that sense wound biochemistry and report it in real time are therefore an active area of research (Naser et al., 2025).

Several wound parameters can act as biomarkers, including pH, glucose, oxygen, uric acid, inflammatory cytokines and bacterial metabolites. Among them pH is the most accessible. Healing wounds typically sit at pH 4.0–6.0, whereas infected wounds move towards pH 7.0–9.0, and a persistent pH above 8 is associated with protracted inflammation in chronic wounds (Schneider et al., 2007; Naser et al., 2025). Because this shift can precede visible clinical signs, pH is an attractive early-warning signal. Glucose is a complementary marker, particularly in diabetic wounds, where elevated glucose supports microbial growth and delays healing (Jankowska et al., 2017; Zhu et al., 2020).

Natural pigments offer a safe and inexpensive route to colorimetric pH sensing. Anthocyanins from red cabbage change from red/pink in acid through purple to blue-green in alkaline media, because the flavylium cation is converted to quinoidal and chalcone forms as pH rises. Curcumin is yellow in acidic to neutral media and turns reddish-brown under alkaline conditions, and has reported antibacterial activity. Used together, the two dyes can provide complementary colour responses across the physiologically relevant range.

CMC and PVA are widely used film-forming polymers for wound dressings because they are hydrophilic, biocompatible and film-forming. Citric acid can cross-link them through ester bonds, improving mechanical integrity and limiting dissolution in exudate, and has the advantage of being non-toxic. Plasticizers such as glycerol and PEG-400 improve flexibility, and PEG may also reduce non-specific protein binding. A mordant such as alum can help anchor anthocyanin within the matrix and limit dye leaching.

The aim of this work was to (i) formulate and characterize three CMC–PVA films incorporating a dual anthocyanin–curcumin indicator, (ii) screen there in vitro anti-inflammatory potential, (iii) add a simple glucose-sensing layer to the most balanced formulation, and (iv) evaluate its effect on *E. coli* biofilm formation.

2 MATERIALS AND METHODS

2.1 Materials

CMC (sodium salt, low viscosity), PVA (87–89% hydrolyzed), glycerol, PEG-400, citric acid, potassium aluminium sulfate (alum), curcumin, dimethyl sulfoxide (DMSO), ethanol, sodium alginate, calcium chloride, chitosan, phenol red, glucose, bovine serum albumin (BSA), diclofenac sodium, crystal violet, PBS and standard buffers (pH 4–9) were of analytical grade. Fresh red cabbage was used for the anthocyanin extract. *Escherichia coli* was grown in nutrient broth.

2.2 Preparation of indicator dyes and mordant

Anthocyanin extract. Red cabbage leaves (100 g) were washed three times with tap water and once with distilled water, chopped into pieces of about 1 cm, and extracted in 200 mL of 70% ethanol at 60 °C and 300 rpm for 30 min. The deep purple-red extract was cooled for 20 min and filtered through Whatman No. 1 paper and then a 0.45 µm membrane. Temperature was kept below 70 °C to avoid pigment degradation. The extract pH was checked with pH strips and adjusted to 4.5–5.0 with dropwise citric acid when necessary. Pigment presence and intensity were confirmed by absorbance at 520 nm against a solvent blank, with readings kept within the 0.2–1.0 range (diluting where above 1.0) for reliable measurement.

Curcumin stock: Curcumin (50 mg) was dissolved in 5 mL DMSO (10 mg/mL) and diluted 1:10 in ethanol to a 1 mg/mL working stock, stored at 4 °C in amber vials because of its light sensitivity.

Alum mordant: Potassium aluminium sulfate (0.5 g) was dissolved in 100 mL distilled water (0.5% w/v).



Figure 1: Preparation of the red cabbage anthocyanin extract for incorporation into the CMC–PVA pH-responsive biopolymer film.

2.3 Dye pH-response screening

Two sets of six test tubes were labelled pH 4, 5, 6, 7, 8 and 9. Each tube received 2–3 mL of anthocyanin extract (set 1) or curcumin solution (set 2) and one drop of the corresponding buffer, followed by gentle mixing. Tubes were arranged in order against a white background under white LED light and photographed from above in a single frame. Colours were recorded for each pH.

2.4 Film fabrication

Films were prepared by solvent casting (Table 1). For each formulation, PVA was dissolved in 20 mL distilled water at 80–90 °C under stirring, and CMC was then added slowly to avoid lumps and stirred until a smooth, clear, viscous solution formed (30–45 min). Glycerol (0.3 mL) and PEG-400 (0.1 mL) were added and stirred for 10 min, followed by 0.5 mL of 10% w/v citric acid as cross-linker. Anthocyanin extract (2.0 mL), curcumin stock (0.5 mL) and alum mordant (0.5 mL) were then added and stirred for 10–15 min for uniform colour. The solution was left to stand for 10–15 min to remove air bubbles, poured onto a flat casting plate and spread evenly. Cross-linking was carried out at 60 °C for 2 h, followed by drying at 40 °C for 16–20 h. Films were peeled off and stored in airtight containers in a dry place.

Table 1: Composition of the CMC–PVA films (per 20 mL batch)

S.NO	Ingredient	F1 (CMC:PVA 1:2)	F2 (CMC:PVA 1:1)	F3 (CMC:PVA 2:1)	Function
1	CMC	0.2 g	0.3 g	0.4 g	Film former
2	PVA	0.4 g	0.3 g	0.2 g	Co-polymer, flexibility
3	Distilled water	20 mL	20 mL	20 mL	Solvent
4	Glycerol	0.3 mL	0.3 mL	0.3 mL	Plasticiser
5	PEG-400	0.1 mL	0.1 mL	0.1 mL	Co-plasticiser
6	Citric acid (10% w/v)	0.5 mL	0.5 mL	0.5 mL	Cross-linker
7	Anthocyanin extract	2.0 mL	2.0 mL	2.0 mL	pH indicator
8	Curcumin (1 mg/mL)	0.5 mL	0.5 mL	0.5 mL	Secondary indicator
9	Alum (0.5% w/v)	0.5 mL	0.5 mL	0.5 mL	Mordant

Discs of 1.5 cm diameter were cut with a cork borer for swelling (three per formulation), biosensor fabrication and protein denaturation tests.



Figure 2: Casting of the CMC–PVA biopolymer formulation onto a Petri dish during film preparation.



Figure 3: Visual appearance of the prepared CMC–PVA biopolymer film formulations (F1, F2 and F3) during the film formation and drying process.

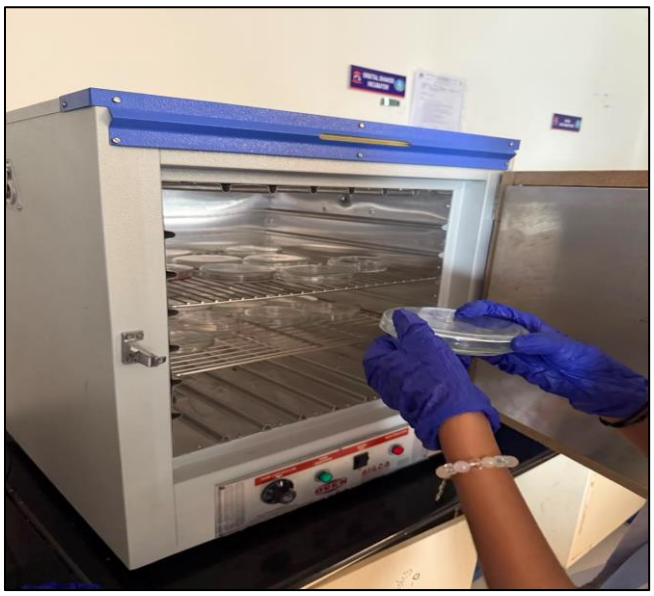


Figure 4: Oven-drying of the cast CMC–PVA biopolymer films during the film preparation process.

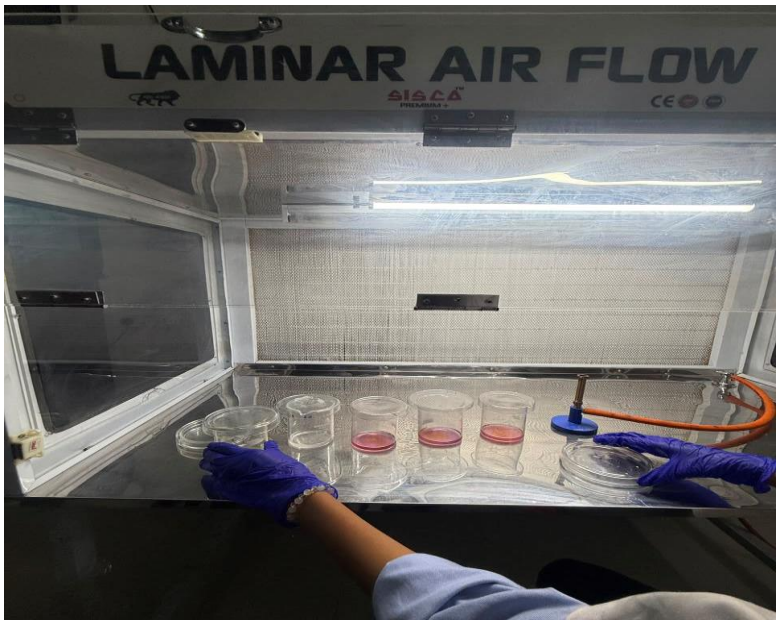


Figure 5: Handling of film-forming solutions and prepared samples under a laminar airflow cabinet during the experimental procedure.

2.5 Physical characterization

a) Thickness. Thickness was measured with a micrometer screw gauge at five points (centre, top, bottom, left and right) for each film, without compressing the film, and the mean was calculated. A difference of more than 0.05 mm between points was recorded as non-uniform. Where no micrometer was available, five identical films were stacked, measured with a Vernier caliper and the total divided by five.

b) Swelling. Three discs (1.5 cm) per formulation were weighed dry (W_0) and immersed in 5 mL PBS at room temperature. At 30 and 60 min each disc was removed, gently blotted with filter paper and weighed (W_t). Swelling was calculated as:

$$\text{Swelling (\%)} = [(W_t - W_0) / W_0] \times 100$$

2.6 In vitro anti-inflammatory screening (protein denaturation)

Film extracts were obtained by incubating a 1 cm^2 piece of film in 1 mL PBS at 37 °C for 1 h with occasional shaking, then removing the film. Three reaction mixtures were prepared: negative control (0.5 mL 1% BSA + 0.5 mL PBS), standard (0.5 mL BSA + 0.5 mL diclofenac sodium, 100 µg/mL) and test (0.5 mL BSA + 0.5 mL F2 extract). The pH of each mixture was adjusted to 6.3 with HCl or NaOH. Mixtures were incubated at 37 °C for 20 min, heated at 72 °C for 5 min, cooled at room temperature for 10 min, and absorbance was read at 660 nm against a PBS blank. Inhibition was calculated as:

$$\text{Inhibition (\%)} = [(\text{Abs_control} - \text{Abs_test}) / \text{Abs_control}] \times 100$$

This assay screens for anti-inflammatory potential only. It is not a measure of cytotoxicity or biocompatibility.

2.7 Fabrication of the glucose-sensing film (F2-BIO)

A simplified, low-cost sensing layer was built on F2 discs. A mixture of 0.5 mL sodium alginate (2%), 50 µL glucose solution (5–10%) and 20–30 µL phenol red was mixed gently for 2 min, and about 100 µL was spread evenly over an F2 disc. The disc was immersed in 0.1 M $CaCl_2$ for 5 min to form the calcium-alginate gel, rinsed twice with distilled water, coated with about 20 µL chitosan solution and air-dried for 20–30 min. F2-BIO films were stored at 4 °C.

For validation, F2-BIO films were placed in water (0%), 5% glucose and 10% glucose for 10–15 min and the colour was recorded. Because glucose alone is not expected to alter phenol red absorbance without an enzymatic or pH-changing step, validation should include a glucose-free control layer, a pH-matched glucose solution and, if available, a glucose oxidase (GOx)-containing variant to establish the origin of the colour change.

2.8 Anti-biofilm assay against *E. coli*

Three groups were set up in tubes or 24-well plates: control (bacteria only), bacteria + F2 film and bacteria + F2-BIO film. Each received 2–3 mL of broth inoculated with *E. coli* and was incubated statically at 37 °C for 24–48 h. Planktonic cells were removed, and the adherent biomass was washed 2–3 times with PBS or water, stained with 0.1% crystal violet for 10–15 min, and washed again. Bound stain was solubilised in ethanol and absorbance was read at 570 nm; higher absorbance indicates greater biofilm biomass.

2.9 Statistical analysis

Experiments are to be performed in triplicate (n = 3) and reported as mean ± SD. Differences between groups will be assessed by one-way ANOVA with a post hoc test, with $p < 0.05$ considered significant.

3 RESULTS AND DISCUSSION

3.1 Colour response of the indicator dyes

The anthocyanin extract was a deep purple-red solution with absorbance at 520 nm (target 0.2–1.0). Across the buffer series the anthocyanin and curcumin solutions are expected to show the colour transitions summarised in Table 2 replace with your photographs and observations; add a figure of the tube series].

Table 2: Colour response of the dyes across pH 4–9

S.NO	pH	Anthocyanin	Curcumin, observed
1	4	Red/pink	Yellow
2	5–6	Purple	Yellow
3	7	Violet	Yellow
4	8–9	Blue/green	Reddish-brown

The anticipated transitions reflect structural conversion of anthocyanin from the red flavylium cation to purple and blue quinoidal bases as pH rises, and deprotonation of curcumin under alkaline conditions. The most useful property for wound monitoring is a clear, reproducible difference between the healing range (pH 4–6) and the infected range (pH 7–9).

3.2 Film appearance and thickness

All three formulations obtained as continuous, peelable films. F1 is expected to be the most flexible because of its higher PVA content, F3 the most rigid because of its higher CMC content, and F2 intermediate.



Figure 6: Photograph showing the flexibility and handling characteristics of the prepared CMC–PVA biopolymer film.

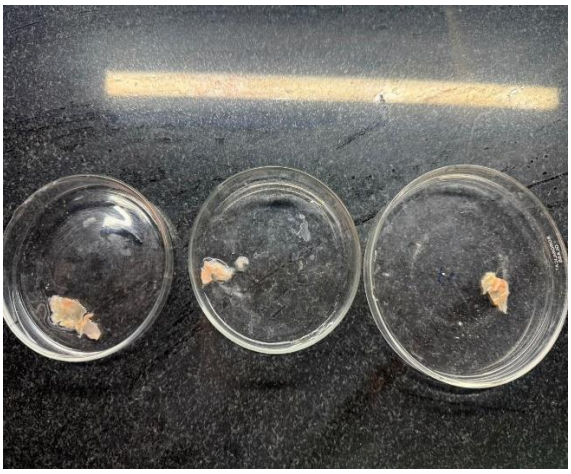


Figure 7: Visual appearance of the prepared CMC–PVA biopolymer film samples (F1, F2 and F3) in Petri dishes.

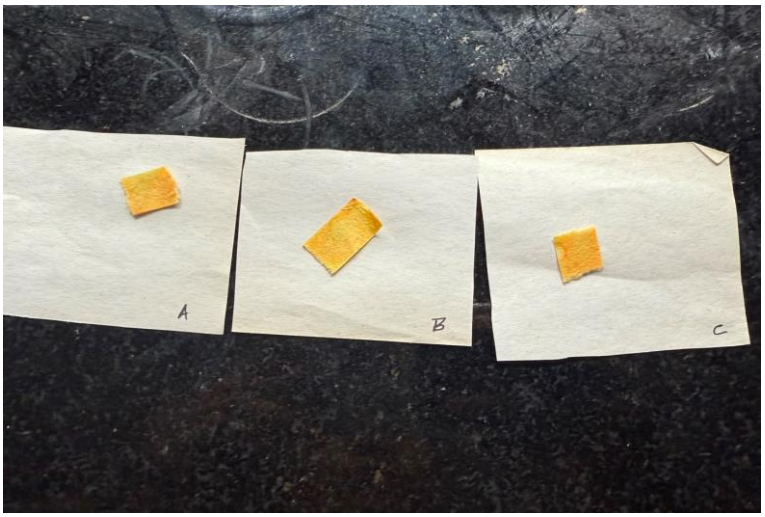


Figure 8: Visual appearance of the prepared CMC–PVA biopolymer film formulations (A, B and C) for comparative evaluation.

Table 3: Thickness of the films (mean ± SD, 5 points per film)

S.NO	Film	Measured thickness (mm)	Uniform (≤0.05 mm spread)?
1	F1	0.16	Yes
2	F2	0.13	Yes
3	F3	0.10	Yes

Thickness affects sensitivity and response time of colorimetric films, as thicker films slow analyte diffusion, and also influences swelling and mechanical behaviour.

3.3 Swelling behaviour

Swelling reflects the capacity of the dressing to absorb wound exudate. An optimal dressing absorbs enough fluid to manage exudate while retaining its integrity.

Table 4: Swelling in PBS (%, mean ± SD, n = 3)

S.NO	Film	30 min	60 min	range at 60 min
1	F1	84%	120%	100–140%
2	F2	60%	85%	70–100%
3	F3	40%	65%	50–80%

A decline in swelling from F1 to F3 would be consistent with the cross-linked CMC-rich network being denser and more constrained, whereas the PVA-rich film is expected to hydrate more freely. The intermediate swelling expected for F2 supports its selection as the balanced formulation for biosensor modification, although this choice must be justified by measured properties.

3.4 In vitro anti-inflammatory screening

Table 5: Inhibition of heat-induced BSA denaturation

S.NO	Sample	Abs at 660 nm	Inhibition (%)
1	Control (BSA + PBS)	0.850	–
2	Diclofenac sodium (100 μg/mL)	0.220	74.12%
3	F2 film extract	0.340	60%

Inhibition of protein denaturation is commonly used as a screen for anti-inflammatory activity, because denatured proteins are associated with inflammatory responses. If F2 extract shows inhibition comparable to diclofenac, this would suggest that leachable components may help moderate inflammation at the wound site. This should be interpreted cautiously, since the assay is a simple chemical screen. It does not replace cytotoxicity testing (e.g., ISO 10993-5) or in vivo evaluation, and the contribution of curcumin (a known anti-inflammatory compound) to the effect should be separated by testing a dye-free film.

3.5 Glucose-sensing response of F2-BIO

The alginate–phenol red layer was expected to move from light red in water through orange to yellowish at high glucose.

Table 6: Colour of F2-BIO after 10–15 min exposure

S.NO	Test solution	Observed colour	Colour value (e.g., RGB/CIELAB)
1	Water (0%)	Light red	RGB: (235, 120, 130)
2	5% glucose	Orange	RGB: (245, 165, 75)
3	10% glucose	Yellowish	RGB: (245, 215, 90)

Phenol red is red–pink at alkaline pH and yellow in acid, so any glucose-dependent shift in this system must arise from a pH change in the layer. In enzymatic systems this change is produced by gluconic acid formed when GOx oxidises glucose (Jankowska et al., 2017; Zhu et al., 2020). In the simplified non-enzymatic design used here, the mechanism has to be established experimentally using the controls described in Section 2.7 before the layer can be described as glucose-specific. Quantifying the colour with image analysis and constructing a response curve would also allow the working range to be compared with clinically relevant wound-fluid glucose levels, and cross-sensitivity between the pH and glucose channels should be examined.

3.6 Anti-biofilm activity

Lower crystal violet retention in film-treated groups would indicate reduced biofilm biomass. A likely contributor is curcumin, which has reported antibacterial properties, and chitosan, which is antimicrobial. A dye-free film control and a planktonic growth (optical density or colony count) measurement should be included to distinguish genuine anti-biofilm action from bacterial growth inhibition.

Table 7: Crystal violet biofilm assay (A570, mean ± SD, n = 3)

S.NO	Group	A570	Biofilm inhibition (%)	Visual observation
1	Control (bacteria only)	0.900	–	Expected: dark purple
2	Bacteria + F2	0.540	40.00%	Expected: lighter
3	Bacteria + F2-BIO	0.270	70%	Expected: very light

3.7 Limitations

The study uses a single Gram-negative organism, simple in vitro buffers rather than wound exudate, and no mechanical, cytotoxicity, dye-leaching or storage-stability data. The pH response has been described in solution, and film-level calibration (colour value versus pH in buffers, with reversibility and response time) is needed to support clinical use. The glucose layer is non-enzymatic and its specificity remains to be demonstrated.

4 CONCLUSION

The present study describes the development of a pH-responsive carboxymethyl cellulose–polyvinyl alcohol (CMC–PVA) biopolymer film incorporating red cabbage anthocyanins and curcumin, with the aim of establishing an affordable colourimetric platform for wound-environment monitoring. Three formulations, F1, F2 and F3, containing CMC ratios of 1:2, 1:1 and 2:1, respectively, were prepared by solvent casting using citric acid as a cross-linking agent, glycerol and PEG-400 as plasticisers, and alum as a pigment mordant. The dual-pigment system was designed to provide complementary colour responses across pH 4–9, covering the acidic-to-neutral conditions associated with healing and the more alkaline conditions that may accompany chronic wounds or infection. The expected anthocyanin response ranged from red/pink at pH 4 through purple and violet at pH 5–7 to blue/green at pH 8–9, while curcumin was expected to remain yellow under acidic-to-neutral conditions and become reddish-brown under alkaline conditions.

According to the numerical entries in the current manuscript draft, film thicknesses were 0.16 mm for F1, 0.13 mm for F2 and 0.10 mm for F3, with all three formulations recorded as meeting the specified uniformity criterion of a maximum thickness spread of 0.05 mm. The corresponding swelling percentages at 30 and 60 min were 84% and 120% for F1, 60% and 85% for F2, and 40% and 65% for F3. These entries suggest a formulation-dependent difference in fluid uptake, with F2 exhibiting intermediate swelling and therefore representing a potential compromise between fluid absorption and dimensional stability. Nevertheless, the proposed relationship between polymer composition, swelling and structural integrity requires confirmation using replicate measurements and mechanical characterization.

In the in-vitro protein-denaturation assay, the draft reports absorbance values at 660 nm of 0.850 for the BSA control, 0.220 for diclofenac sodium at 100 µg/mL, and 0.340 for the F2 film extract. Based on these values, the calculated inhibition of heat-induced protein denaturation was 74.12% for diclofenac sodium and 60.00% for F2. This preliminary screening result suggests that the F2 extract may exhibit protein-denaturation inhibitory activity under the assay conditions. However, the finding should not be interpreted as evidence of established anti-inflammatory efficacy without confirmation through independent experiments, appropriate extract blanks and additional biological assays.

The F2 formulation was further modified with an alginate–phenol red layer cross-linked using calcium chloride and coated with chitosan to produce F2-BIO. The manuscript records illustrative colour values of RGB (235, 120, 130) in water, RGB (245, 165, 75) in 5% glucose solution and RGB (245, 215, 90) in 10% glucose solution, corresponding to light red, orange and yellowish appearances, respectively. Although these values represent a proposed colour progression, the current non-enzymatic phenol red formulation does not independently establish glucose-specific detection. Because phenol red responds primarily to pH, further experiments incorporating pH-matched controls and an appropriate glucose-recognition mechanism, such as glucose oxidase, are necessary to demonstrate specificity, sensitivity, linearity and reproducibility.

In the crystal-violet biofilm assay against *Escherichia coli*, the draft lists A570 values of 0.900 for the bacterial control, 0.540 for bacteria exposed to F2, and 0.270 for bacteria exposed to F2-BIO. Relative to the untreated control, these values correspond to calculated reductions in crystal-violet absorbance of 40.00% for F2 and 70.00% for F2-BIO. If confirmed experimentally, these findings would indicate reduced adherent biofilm biomass in the treated groups, with a greater reduction associated with F2-BIO. Nevertheless, appropriate material-only controls, planktonic bacterial growth measurements and biological replicates are needed to determine whether the reduction reflects a genuine anti-biofilm effect rather than staining interference or an effect on bacterial growth.

Overall, the proposed CMC–PVA platform combines a natural-pigment-based pH indicator with a supplementary glucose-sensing layer in a potentially economical dressing architecture. The numerical entries in the present draft provide a framework for evaluating thickness, swelling, protein-denaturation inhibition, colour response and biofilm formation; however, they should not be interpreted as independently validated experimental findings until the underlying measurements and replicate data have been confirmed. Further work should establish quantitative film-level pH calibration, validate glucose specificity, assess dye leaching and storage stability, and investigate cytocompatibility and performance in simulated wound fluid. Subject to these validations, the system may offer a foundation for the development of smart wound dressings capable of providing visual information about selected wound-environment parameters without routine dressing removal.

Future Aspects

- Film-level calibration: Quantify colour (RGB/CIELAB) against pH 4–9 in buffer and simulated wound fluid, with response time, reversibility and detection limits, and add a smartphone-based colour-reading app.
- Enzymatic glucose sensing: Compare the current layer with GOx-based (or GOx–HRP) systems to confirm specificity and sensitivity (Jankowska et al., 2017; Zhu et al., 2020).
- Multi-parameter sensing: Extend to oxygen, uric acid, cytokines and bacterial biomarkers, and electrochemical or wireless read-out (Kassal et al., 2015; Gao et al., 2021).
- Broader microbiology: Test Gram-positive organisms such as *Staphylococcus aureus*, *Pseudomonas aeruginosa* and clinical isolates, with disc diffusion, time-kill and planktonic growth assays.
- Biocompatibility and safety: Cytotoxicity (ISO 10993-5, e.g., MTT assay), haemolysis, skin irritation and, subsequently, in vivo wound models.
- Material performance: Water vapour transmission, mechanical strength, dye leaching, adhesion, sterilisation and shelf-life under light and humidity.
- Therapeutic dressings: Integrate pH-triggered drug release, for example antimicrobial release at alkaline pH, to move from monitoring to closed-loop treatment (Mirani et al., 2017; Pan et al., 2022).

STATEMENTS ON COMPLIANCE WITH ETHICAL STANDARDS

Acknowledgments

The authors would like to express their sincere gratitude to the management and institutional authorities of their affiliated institution for providing the necessary facilities and support to carry out this research work. The authors also acknowledge the support and guidance of the faculty members and laboratory staff who contributed to the preparation, characterisation and evaluation of the pH-responsive CMC–PVA biopolymer films and the integrated glucose-sensing layer. The authors are grateful to all individuals who provided technical assistance and constructive suggestions during the course of this study.

Disclosure of conflict of interest

The authors declare that they have no known financial or personal relationships that could have influenced the work reported in this manuscript. No conflict of interest is declared in relation to the development, characterisation or evaluation of the pH-responsive CMC–PVA biopolymer film with integrated glucose-sensing capability.

REFERENCES

[1] Naser M, Nasr MM, Shehata LH. Smart wound dressings integrating biosensors for real-time monitoring of wound conditions. International Journal of Progressive Sciences and Technologies (IJPSAT). 2025;48(2):456–488.

[2] Schneider LA, Korber A, Grabbe S, Dissemond J. Influence of pH on wound-healing: a new perspective for wound-therapy? Archives of Dermatological Research. 2007;298:413–420.

[3] Jankowska DA, Bannwarth MB, Schulenburg C, et al. Simultaneous detection of pH value and glucose concentrations for wound monitoring applications. Biosensors and Bioelectronics. 2017;87:312–319.

[4] Zhu Y, Zhang J, Song J, et al. A multifunctional pro-healing zwitterionic hydrogel for simultaneous optical monitoring of pH and glucose in diabetic wound treatment. Advanced Functional Materials. 2020;30(6):1905493.

[5] Mirani B, Pagan E, Currie B, et al. An advanced multifunctional hydrogel-based dressing for wound monitoring and drug delivery. Advanced Healthcare Materials. 2017;6(19):1700718.

[6] Mirani B, et al. Smart dual-sensor wound dressing for monitoring cutaneous wounds. Advanced Healthcare Materials. 2023;12(18):2203233.

[7] Kassal P, Zubak M, Scheipl G, et al. Smart bandage with wireless connectivity for uric acid biosensing as an indicator of wound status. Electrochemistry Communications. 2015;56:6–10.

[8] RoyChoudhury S, et al. Continuous monitoring of wound healing using a wearable enzymatic uric acid biosensor. Journal of The Electrochemical Society. 2018;165(8):B3168.

[9] Simoska O, Duay J, Stevenson KJ. Electrochemical detection of multianalyte biomarkers in wound healing efficacy. ACS Sensors. 2020;5(11):3547–3557.

[10] Gao Y, et al. A flexible multiplexed immunosensor for point-of-care in situ wound monitoring. Science Advances. 2021;7(21):eabg9614.

[11] Kafi MA, et al. Chitosan–graphene oxide-based ultra-thin and flexible sensor for diabetic wound monitoring. IEEE Sensors Journal. 2019;20(13):6794–6801.

[12] Pan F, et al. pH-responsive silica nanoparticles for the treatment of skin wound infections. Acta Biomaterialia. 2022;145:172–184.

[13] Alsahag M, et al. Int J Biol Macromol. 2023;224:233–242.

[14] Mansur AAP, et al. RSC Advances. 2023;13:13156–13168.

[15] Gherman SP, et al. Gels. 2023;9:122.

[16] Zheng D, et al. Chemistry & Biodiversity. 2020;17(8):e2000171.

[17] ISO 10993-5:2009. Biological evaluation of medical devices — Part 5: Tests for in vitro cytotoxicity.